



Plasma flows, Birkeland currents and auroral forms in relation to the Svalgaard-Mansurov effect

P. E. Sandholt¹ and C. J. Farrugia²

¹Department of Physics, University of Oslo, Oslo, Norway

²Space Science Center, University of New Hampshire, Durham, USA

Correspondence to: P. E. Sandholt (p.e.sandholt@fys.uio.no)

Received: 2 February 2012 – Revised: 17 April 2012 – Accepted: 18 April 2012 – Published: 9 May 2012

Abstract. The traditional explanation of the polar cap magnetic deflections, referred to as the Svalgaard-Mansurov effect, is in terms of currents associated with ionospheric flow resulting from the release of magnetic tension on newly open magnetic field lines. In this study, we aim at an updated description of the sources of the Svalgaard-Mansurov effect based on recent observations of configurations of plasma flow channels, Birkeland current systems and aurorae in the magnetosphere-ionosphere system. Central to our description is the distinction between two different flow channels (FC 1 and FC 2) corresponding to two consecutive stages in the evolution of open field lines in Dungey cell convection, with FC 1 on newly open, and FC 2 on old open, field lines. Flow channel FC 1 is the result of ionospheric Pedersen current closure of Birkeland currents flowing along newly open field lines. During intervals of nonzero interplanetary magnetic field B_y component FC 1 is observed on either side of noon and it is accompanied by poleward moving auroral forms (PMAFs/prenoon and PMAFs/postnoon). In such cases the next convection stage, in the form of flow channel FC 2 on the periphery of the polar cap, is particularly important for establishing an IMF B_y -related convection asymmetry along the dawn-dusk meridian, which is a central element causing the Svalgaard-Mansurov effect. FC 2 flows are excited by the ionospheric Pedersen current closure of the northernmost pair of Birkeland currents in the four-sheet current system, which is coupled to the tail magnetopause and flank low-latitude boundary layer. This study is based on a review of recent statistical and event studies of central parameters relating to the magnetosphere-ionosphere current systems mentioned above. Temporal-spatial structure in the current systems is obtained by ground-satellite conjunction studies. On this point we emphasize the important informa-

tion derived from the continuous ground monitoring of the dynamical behaviour of aurora and plasma convection during intervals of well-organised solar wind plasma and magnetic field conditions in interplanetary coronal mass ejections (ICMEs) during their Earth passage.

Keywords. Ionosphere (Plasma convection) – Magnetospheric physics (Polar cap phenomena; Solar wind-magnetosphere interactions)

1 Introduction

The ground magnetic disturbances in the polar cap related to the sector structure of the interplanetary magnetic field (IMF) (B_x polarity regimes in the Parker spiral configuration of the magnetic field embedded in the solar wind) were first identified by Svalgaard (1968) and Mansurov (1969). The azimuthal (B_y) component of the IMF was later demonstrated to be the cause of this behaviour (Friis-Christensen et al., 1972). The effect is characterised by an enhanced H-component deflection in away ($B_x < 0$; $B_y > 0$) sectors and a decreased H-component in toward ($B_x > 0$; $B_y < 0$) sectors (Svalgaard, 1973). A good illustration of this effect at station Thule is given in Janzhura and Troshichev (2011) (see their Fig. 5).

The traditional interpretation of this so-called Svalgaard-Mansurov (S-M) effect is in terms of the IMF B_y related dawn-dusk convection asymmetry which is produced by magnetic tension forces acting on newly open field lines, as depicted by Jørgensen et al. (1972) (see their Fig. 1).

The aim of this paper is to argue that this interpretation is incomplete. As a supplement to the traditional view, we point out the importance of ionospheric Pedersen current closure of

two sets of field-aligned currents (four-sheet FAC system; see e.g., Potemra, 1994, and Anderson et al., 2008, their Fig. 5) connecting the magnetopause and the ionosphere in two consecutive phases of evolution of open field lines, i.e., newly open and old open field lines. In the latter stage the open field lines are connected to solar wind-magnetosphere dynamo action in the high-latitude boundary layer, on the downstream side of the cusp.

Our contention is that the ionospheric Hall current associated with the ionospheric Pedersen current closure of the field-aligned current pair in the second stage of open field line evolution mentioned above, which we call C1-C2 currents, is a further important source of the S-M effect. Our study is inspired by new information relating to the S-M effect that has been reported in recent years. Among these new sources of information is a large statistical study of ground magnetic deflections as a function of the IMF orientation that has recently been published by Weimer et al. (2010). This is a comprehensive overview of ground magnetic perturbations plotted in MLAT/MLT coordinates corresponding to the different IMF strengths and orientations in the GSM Y-Z plane (the clock angle). It is based on a large database of magnetic recordings from many magnetometer chains around the globe. From this Weimer et al. pattern of magnetic perturbations we are able to extract essential information on IMF B_y -related plasma convection and the associated S-M effect.

The second source of new information for this study is a series of ground-satellite conjunction studies of spatial-temporal structure of configurations of aurora/precipitation, FAC and plasma convection in relation to IMF orientation. It was in view of these studies that we find it appropriate to distinguish between distinct stages and spatial structures (flow channels) in the evolution of open field lines in Dungey cell convection. As a matter of nomenclature, we refer to the flow channels on newly open and old open field lines as FC 1 and FC 2, respectively. The FC 1 channel is bordered by a pair of FACs which is closely connected to the dynamic auroral forms that are often referred to as poleward moving auroral forms (PMAFs). These specific auroral forms are observed on either side of the “midday gap aurora” near noon and are moving noonward and poleward (Sandholt and Farrugia, 2007a) in the precipitation regimes called dayside boundary plasma sheet (BPS), low-latitude boundary layer (LLBL), cusp and mantle (Lockwood, 1997; Sandholt et al., 2004, 2002). The source mechanism is pulsed magnetopause reconnection, called flux transfer events (Russell and Elphic, 1978).

Flow channel FC 2, appearing in the subsequent stage of anti-sunward convection at the polar cap boundary, on the downstream side of the cusp, is located in the regimes of mantle and polar rain precipitations. This flow is related to the ionospheric Pedersen current closure of the Birkeland currents we call C1-C2 (Sandholt and Farrugia, 2009). C2 is the poleward part of the R1 current which maps to the outer part of the flank LLBL (see e.g., Sonnerup and Siebert,

2003). This is the “extra downstream cleft-associated R1 current” of Watanabe et al. (1996). C1 is a more distributed (latitudinally wider) current in the polar cap which is connected to the tail magnetopause current (Sandholt and Farrugia, 2009). This is the “extra R0 current” of Watanabe et al. (1996).

The distinction we make between the adjacent R1 and C2 currents, being associated with different ionospheric flow channels (FC 1 versus FC 2) in different stages of the convection cycle, is supported by plasma and magnetic field observations in the ground-satellite conjunction studies of Sandholt and Newell (1992) and Farrugia et al. (2004). Our view is also consistent with the sequential activations of flow channels FC 1 and FC 2 clearly seen during the first 20 min of the convection cycle in response to rapid southward turnings of the IMF (Sandholt et al., 2010a). Both these aspects will be demonstrated below.

The spatial-temporal structure in Dungey cell convection described above is, furthermore, supported by the different spatial polar cap convection regimes appearing in response to strong forcing by well-organized magnetic fields in interplanetary CMEs, i.e., the periphery versus the centre of the polar cap. In the centre of the polar cap, the dayside source of polar cap convection saturates at speeds of $0.8\text{--}1.0\text{ km s}^{-1}$ (Troshichev et al., 2000). This is in contrast to the higher ($1\text{--}2\text{ km s}^{-1}$) speeds of anti-sunward convection that are observed along the periphery of the polar cap, on the dawn (for IMF $B_y > 0$ cases) and dusk (for $B_y < 0$ cases) sides.

When we combine these new perspectives on plasma convection, field-aligned currents, aurora and ground magnetic deflections, we arrive at an updated interpretation of the Svalgaard-Mansurov effect which we shall describe in this study.

We also point out that the S-M effect is often considered to be a summer phenomenon (see Janzhura and Troshichev, 2011, and references therein). Our first example confirms the winter-summer asymmetry, but also documents the presence of a smaller, but non-negligible effect even in winter.

In the case examples reported below, we shall take advantage of the well-organized behaviour of magnetic fields in certain interplanetary CMEs (Burlaga et al., 1981; Lepping et al., 2003), during their Earth passage.

2 Case 1 (ICME): 30 November 1979; Svalgaard-Mansurov effect in Arctic and Antarctic magnetograms

As an introduction to the phenomenon of the S-M effect, we present an example of the response in the ground magnetic field in the dayside polar cap, poleward of the cusp, in both hemispheres. This occurred at the time of an event showing a rapid magnetic field B_y polarity shift in an interplanetary CME that passed Earth on 30 November 1979. The source of this event is the first coronal transient directed towards

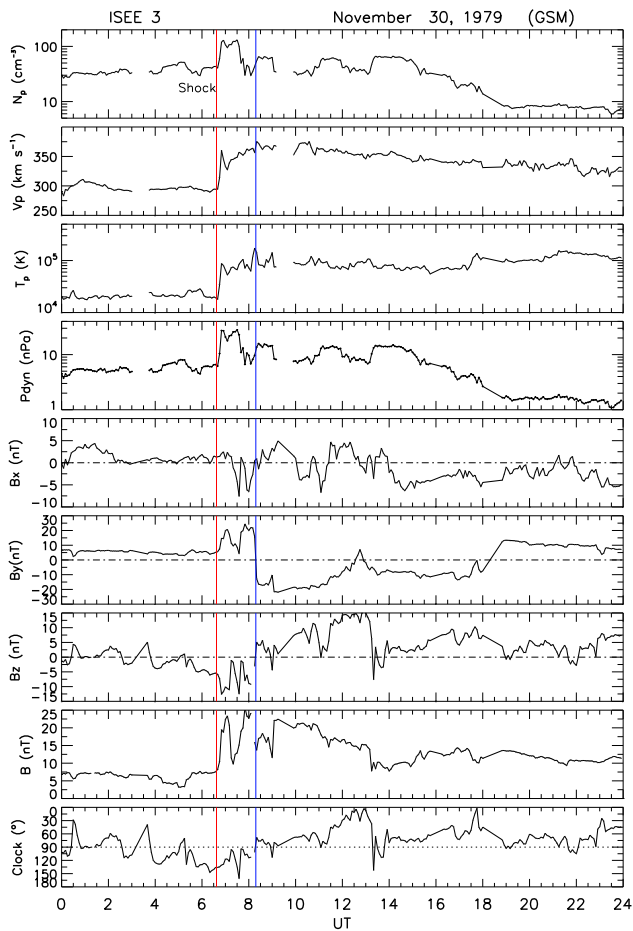


Fig. 1. ISEE 3 data for 30 November 1979: panels from top to bottom show proton density, bulk speed, temperature, dynamic pressure, magnetic field components B_x , B_y , B_z in GSM coordinates, the total field and the clock angle in the GSM Y-Z plane. The arrival of an interplanetary (IP) shock at approx. 06:35 and the abrupt B_y polarity change at approx. 08:20 UT are marked by vertical guidelines.

Earth that was observed by the satellite-borne coronagraph Solwind on 27 November 1979 (Howard et al., 1982).

Figure 1 shows ISEE 3 data for 30 November 1979. At 12:00 UT on this day ISEE 3 was at $(196, 58, -12) R_E$. It is, thus, somewhat distant from the Sun-Earth line. However, correlation lengths of ICMEs are $> 50 R_E$ from the Sun-Earth line (Farrugia et al., 2005). The red vertical guideline marks the arrival of an IP shock at 06:35 UT. The sheath plasma behind the shock is characterised by enhanced density, speed, proton temperature, dynamic pressure, a large (factor 3) B-field compression and a fluctuating south-east ($B_z < 0$; $B_y > 0$) directed field. This is a slow ICME. An abrupt change in B_y polarity from positive to negative occurred at approx. 08:20 UT, at the leading edge of the transient. The next interval (08:20–12:00 UT) is characterised by a B_y -dominant field (B_y : -20 to -10 nT).

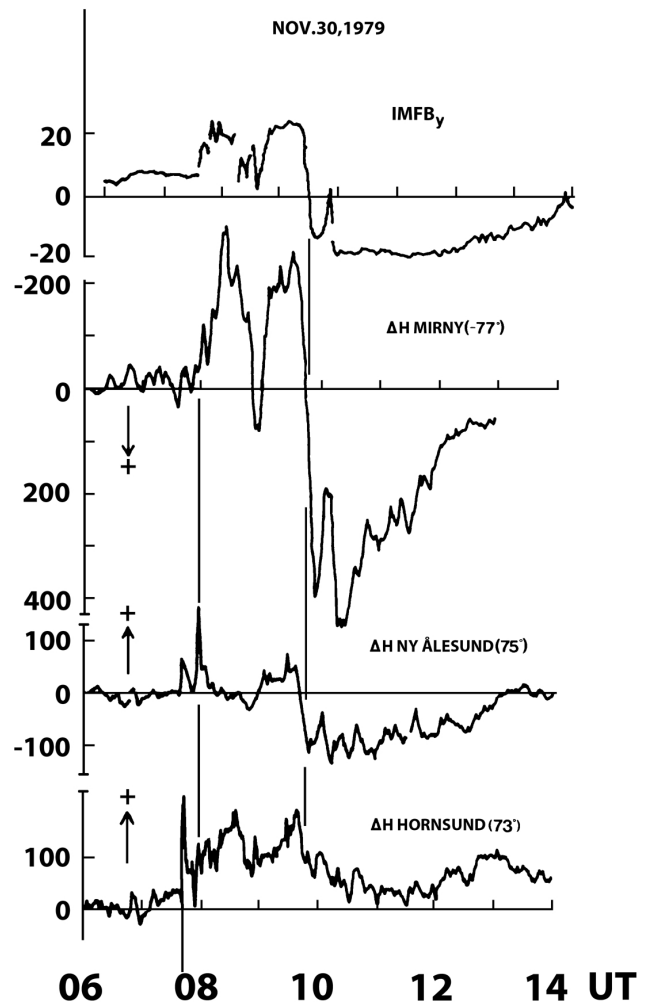


Fig. 2. Panels from top to bottom shows the magnetic field B_y (east-west component) trace obtained from spacecraft ISEE 1, and H-component of the ground magnetic deflections from stations in Antarctica (Mirny; -77° MLAT) and the Arctic stations Ny Ålesund (75° MLAT) and Hornsund (74° MLAT) on Svalbard. The ISEE trace is displaced forward by approx. 15 min.

We note that the arrival of the interplanetary (IP) shock caused an abrupt cusp auroral brightening at 07:40 UT, followed by a series of brightenings/poleward-moving auroral forms, as reported by Sandholt et al. (1985). The main focus here is on the two intervals of different B_y polarities during 06:35–08:20 and 08:20–12:00 UT, separated by the sharp B_y polarity shift at 08:20 UT. As we shall see, the Svalgaard-Mansurov effect is observed under both these B_y -polarity regimes. We recognise that, although $B_z > 0$ after the B_y polarity shift, the clock angle remains large enough for subsolar reconnection to be ongoing until 11:30 UT (ISEE 3 time).

Figure 2 shows the association between variations in the B_y component of the ICME field detected by ISEE 1 and ground magnetic deflections at polar cap stations in both hemispheres (Svalbard and Mirny). Svalbard and Mirny are

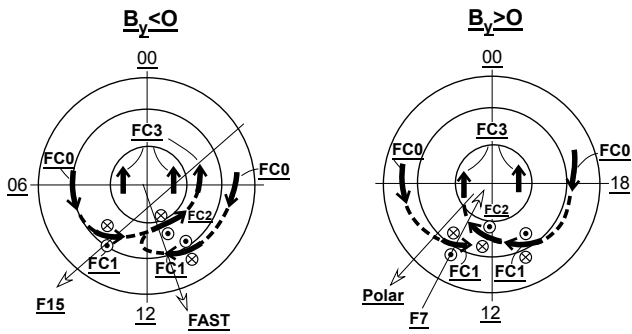


Fig. 3. Schematic illustration of ionospheric plasma flow channels FC 0, FC 1, FC 2 and FC 3 in MLT/MLAT coordinates as extracted from the statistical ground magnetic perturbations of Weimer et al. (2010). Flow patterns for southwest ($B_y < 0$) and southeast ($B_y > 0$) IMF orientations are shown in the left and right-side panels, respectively. The polarities of paired FAC sheets associated with the FC 1 and FC 2 ionospheric flows are indicated. Also shown are specific tracks of satellites (DMSP F15, FAST, Polar and DMSP F7) used to document the FAC and plasma configurations.

conjugate positions. At 12:00 UT on this day ISEE 1 was located in the magnetosheath at (14, -15 , 0) R_E (GSE coordinates).

The essential observation is the correspondence between the B_y polarity shift recorded by ISEE 1 at $\sim 09:30$ UT (70 min after ISEE 3) and the ground magnetic signature at $\sim 09:45$ UT. The ISEE 1 trace is displaced forward by ~ 15 min in order to line up these transitions in the satellite and ground data.

In the H-component deflection trace at the polar cap stations the central features of the B_y -trace recorded by ISEE-1 between 08:00–12:00 UT are reproduced. The response is particularly clear in Mirny, Antarctica (12:00 MLT = 08:33 UT). This illustrates the directly driven nature of the solar wind – magnetosphere – ionosphere coupling in this case. The physics of this coupling is the topic of this article.

In particular we notice the ground response, in both hemispheres, to the rapid change of IMF B_y polarity from positive to negative recorded by ISEE 1 at approx. 09:30 UT. This is a clear illustration of the Svalgaard-Mansurov effect. In our model this is a result of the ionospheric Pedersen current closure of a specific pair of Birkeland currents connecting the magnetopause and the ionosphere, as described below. The Hall current excited by the E -field associated with the Pedersen current closure gives rise to the ground magnetic deflection. The latter association is as described by Fukushima (1969).

We observe that the S-M effect is larger in the summer hemisphere (Mirny, Antarctica) compared to the winter hemisphere (Ny Ålesund and Hornsund, Svalbard), as expected because of the conductivity difference.

3 Svalgaard-Mansurov effect in Weimer patterns of ground magnetic perturbations

Figure 3 shows a schematic drawing of plasma flow channels FC 0, FC 1, FC 2 and FC 3 as equivalent ionospheric convection extracted from the statistical ground magnetic perturbations of Weimer et al. (2010). The coordinate system is magnetic local time (MLT) versus magnetic latitude (MLAT). These flow channels correspond to distinct, successive stages of Dungey cell convection as open field lines are transported poleward and duskward for IMF $B_y < 0$ and poleward and dawnward for IMF $B_y > 0$, i.e., newly open (FC 1) and old open field lines (FC 2), and flow channels at the dawn-dusk boundaries of the polar cap driven by magnetotail reconnection (FC 3). FC 0 represents the sunward return flow at lower latitudes, on closed field lines. Contrary to the more moderate (≤ 1 km s^{-1}) anti-sunward flows in the centre of the polar cap (Troshichev et al., 2000) the flow channels along the periphery of the polar cap (FC 2 and FC 3) are characterised by speeds of 1–2 km s^{-1} (Sandholt and Farrugia, 2009; Andalsvik et al., 2012). In this article, we shall place focus on the FC 1 and FC 2 channels. Contrary to FC 1 and FC 2, flow channels FC 3 are associated with substorm activity driven by magnetotail reconnection, as recently documented by Andalsvik et al. (2012). It is, however, also a phase of the Dungey cycle – an even later one – distinguished by closure of open flux in the tail and its return to the dayside avoiding wholesale erosion.

From Fig. 3 it seems that the S-M effect in the polar cap, on the downstream side of the cusp, is mainly manifested by the presence of positive (negative) X-component (north–south) ground magnetic deflections in the regimes of flow channels FC 2 corresponding to positive (negative) IMF B_y polarities, respectively. Flow channels FC 1 (newly open field lines), on the other hand, give rise to X-deflections of opposite polarities on either side of noon and at lower latitudes for a given B_y polarity. This result is supported by the relevant data we shall report below.

Birkeland current configurations relating to flow channels FC 1 and FC 2 are also indicated in Fig. 3 (see also Anderson et al., 2008). This is based on the observation that both these flows result from the ionospheric Pedersen current closure of FAC pairs. This association has been demonstrated in previous ground-satellite conjunction studies (see below). A basic element of our description is that we distinguish between flows on newly open (FC 1) and old open field lines (FC 2), i.e., those corresponding to the two first stages of the evolution of open flux in Dungey cell convection initiated by magnetopause reconnection. FC 2 is related to the Pedersen current closure of the the Birkeland current pair we shall refer to as C1 (northernmost) and C2, as in our previous studies. These FACs (C1 and C2) are discussed by Watanabe et al. (1996). According to Watanabe et al. (1996) C1 is the “extra region 0 current” which is connected to the

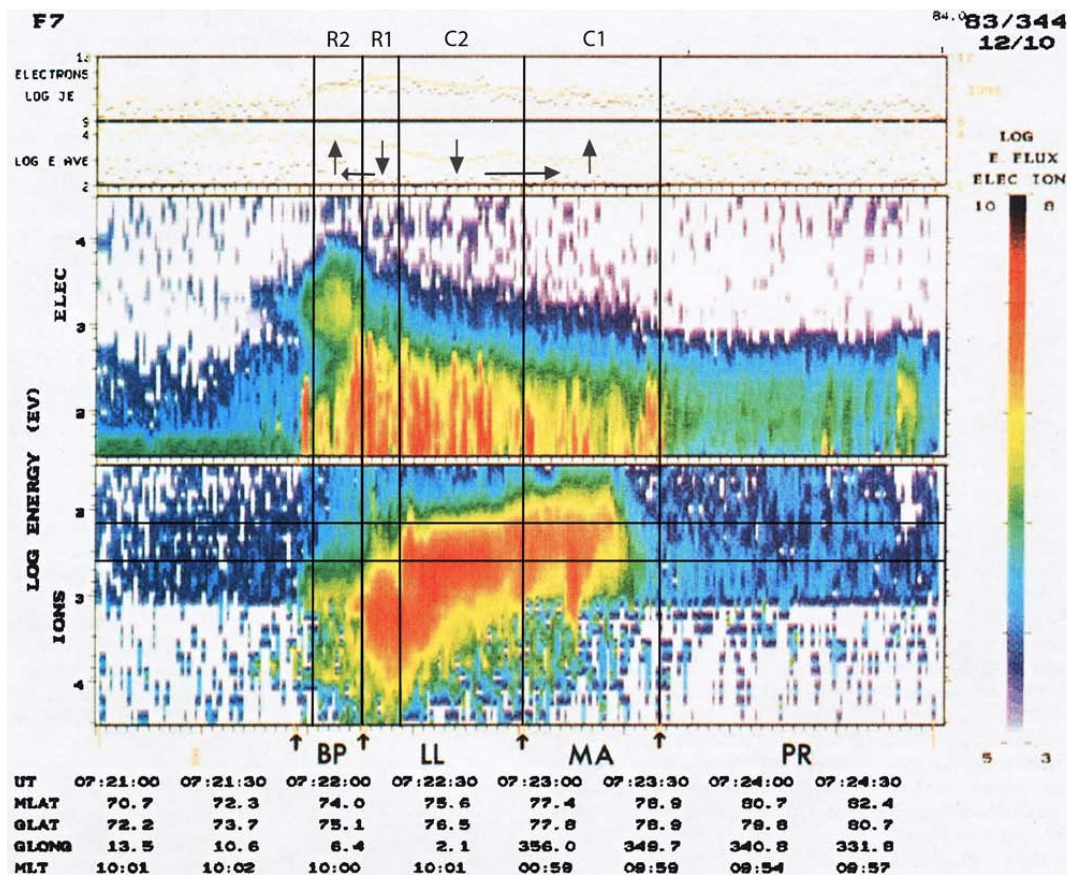


Fig. 4. DMSP F7 data particle precipitation data (electrons and ions) during a north-bound pass along the 10:00 MLT meridian in the cusp/cleft region. Four FAC regimes (R2-R1-C2-C1) are marked in the figure. The corresponding precipitation regimes are marked BP (boundary plasma sheet), LL (LLBL-1 and LLBL-2), and MA (mantle). The satellite track is indicated in Fig. 3.

tail magnetopause and C2 is the “extra downstreamside cleft-associated region 1 current”.

We note that the C1-C2 current system was predicted on the basis of auroral observations by Sandholt et al. (1992) (see also Denig et al., 1993). It later appears in the systematic FAC study of Taguchi et al. (1993) in a steady-state reconnection scenario, as their LCC-HCC currents.

Below we shall illustrate the association between the four-sheet FAC configuration and associated particle precipitation regimes for the DMSP F7 pass in the $B_y > 0$ /prenoon case as marked in Fig. 3.

A four-sheet Birkeland current configuration appears in the prenoon sector for $B_y > 0$ ($B_z < 0$) conditions and in the postnoon sector in the $B_y < 0$ ($B_z < 0$) case. Both these configurations have been documented in previous ground-satellite conjunction studies. The data from the pass by the Polar spacecraft at mid-altitudes along the 09:00 MLT meridian, marked in Fig. 3, are shown in Farrugia et al. (2003). The four sheets of latitudinally separate FACs, ion/electron plasma regimes, and auroral forms were identified. Here (Fig. 4) we show a representative example of the particle precipitation and FAC configuration along the 10:00 MLT

meridian in the $B_y > 0$ ($B_z < 0$) case, as obtained by spacecraft F7.

Essential elements are: (i) a four-sheet FAC system (C1-C2-R1-R2 from north to south) is shown in relation to (ii) particle precipitation (electrons and ions) and (iii) auroral observations from the ground (Svalbard MSP data) along the 10:00 MLT meridian. The subdivision of different FAC regimes is done based on the satellite magnetic field observations (not shown) given in Fig. 4a in Sandholt and Newell (1992).

The important thing for us here is that the Region 1 current is split in two components: our R1 and C2 currents. FAC R1 is coupled to the R2 current located further south, while C2 is connected to C1 (via ionospheric Pedersen current closure, as indicated by arrows). The split of R1 in two parts is, furthermore, emphasized by the jump in the ion low-energy cutoff, i.e., which we interpret as a discontinuity in time elapsed since magnetopause reconnection (see e.g., Lockwood et al., 1993). The two low-energy ion cutoffs are marked by horizontal lines in the ion precipitation panel in Fig. 4. This is the so-called staircase (or stepped) cusp precipitation (Escoubet et al., 1992). We conclude from these observations

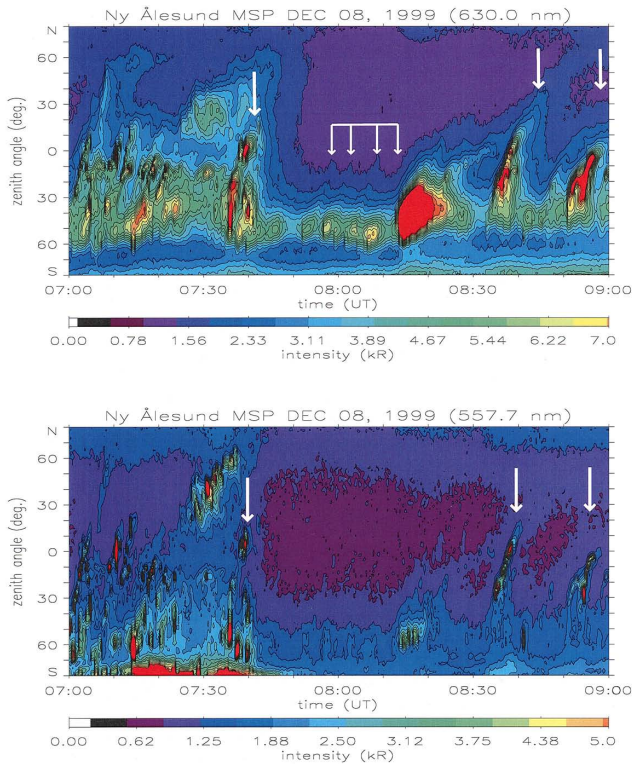


Fig. 5. MSP observations of auroral configuration around magnetic noon on 8 December 1999. Line-of-sight intensities are shown as a function of zenith angle for the red (top panel) and green oxygen lines at 630.0 and 557.7 nm. North is up. PMAF/prenoon (07:40 UT) and PMAFs/postnoon (08:35–09:00 UT) are marked by arrows.

that the two R1 components (R1 and C2) belong to two different phases of evolution of open field lines: newly open flux (R1 and FC 1 channel) and old open field lines (C2 and FC 2). The circuit involving the C1–C2 currents and their ionospheric closure current gives rise to flow channel FC 2. This type of two-component R1 FAC configuration (R1 and C2) is also illustrated in the recent statistical study of Wing et al. (2010) (see their Fig. 7).

The mid-altitude data obtained during the Polar pass marked in Fig. 3 (IMF $B_y > 0$ /prenoon case) shows a four-sheet FAC configuration (C1–C2–R1–R2) in relation to plasma data and auroral observations from the ground (Svalbard MSP data). The complete dataset is given in Farrugia et al. (2003).

Data from the FAST spacecraft obtained during the traversal along the postnoon meridian (13:00 MLT) marked in Fig. 3 ($B_y < 0$ /postnoon case) document the four-sheet FAC current system (C1–C2–R1–R2) in relation to a staircase particle precipitation in the cusp region (Farrugia et al., 2004). This pass occurred during an interval of stable $B_y < 0$ conditions (clock angle near 135° lasting for many hours around

the time of the pass). Flow channels FC 1 and FC 2 were documented by ground radars SuperDARN and Sondrestrom.

4 Cases 2–5

4.1 FC 1–FC 2 flows: Aurora-FACs-convection configurations

Below we shall report representative examples of aurora-FAC-convection configurations associated with the FC 1–FC 2 flow channels indicated schematically in Fig. 3. The temporal evolution of flow channel events are monitored from ground magnetometers.

4.1.1 Case 2: Auroral configuration across noon ($B_y > 0$); prenoon versus postnoon asymmetry (8 December 1999)

Figure 5 shows meridian scanning photometer (MSP) observations of the red (630.0 nm) and green (557.7 nm) line auroral emissions when the station at Ny Ålesund moved with the Earth from the prenoon side (07:00 UT) via noon (08:40 UT) to the postnoon side on 8 December 1999. We shall emphasize the pre-noon versus post-noon asymmetry evident in the cusp region auroral configuration. We attribute this to the asymmetry in FACs shown in Fig. 3. Here we consider the configuration for the prevailing $B_y \geq 0$ conditions. Returning to the schematic FAC illustration in Fig. 3 the prenoon side events are characterised by four latitudinally separate FAC sheets located on either side of the FC 1 and FC 2 flows. This is different from the post-noon side events where only two sheets are present. We shall look for this prenoon versus postnoon asymmetry in the auroral observations.

Moving from left to right, we notice the following three features of the auroral configuration: (i) prenoon aurora consisting of a multi-layered latitudinal structure when moving from south to north: (a) green line diffuse aurora (CPS source) at the equatorward boundary of the MSP field of view (FOV) until 07:40 UT, (b) PMAFs/prenoon activity (dayside BPS source) (white arrow); (ii) red-dominated cusp-type aurora (“midday gap” aurora) during the interval 07:41–08:30 UT, and (iii) two consecutive poleward-moving forms (PMAFs/postnoon) in the interval 08:35–09:00 UT (two white arrows).

We shall argue that the 07:40 UT aurora, which belongs to our category PMAFs/prenoon/ $B_y > 0$, corresponds to FAC structure in FC 1/prenoon/ $B_y > 0$ in Fig. 3. In this case, the initial brightening stage of the PMAFs is captured by the MSP. This is contrary to the two auroral forms marked in the interval 08:35–09:00 UT, which correspond to our category PMAFs/postnoon/ $B_y > 0$. As documented in Sandholt et al. (2004), they originate in the postnoon sector (outside the MSP FOV) and, in our view, the present MSP signature corresponds to a later phase of PMAF evolution (notice the higher latitude of the entrance to the MSP FOV). This stage

is somewhere in the transition phase between flow channels FC 1 and FC 2, as indicated in Fig. 3.

In the present case, the configuration of PMAFs/prenoon–midday gap aurora – PMAFs/postnoon was accentuated by certain changes in the IMF orientation (southeast before 07:40 and after 08:30 UT while strongly south in the interval 07:40–08:30 UT). The same type of PMAFs/prenoon versus PMAFs/postnoon asymmetry under steady south-east IMF conditions has been documented in Sandholt and Farrugia (2007b).

We conclude that the asymmetry across noon in PMAFs/prenoon versus PMAFs/postnoon reflects the asymmetry across noon of the FC 1-FC 2 flows and associated FAC configuration described in Fig. 3. The prenoon FAC structure spans a wider latitudinal range than the postnoon structure, as does the auroral activity. The PMAFs we refer to are explained in terms of the evolution of open flux tubes initiated by flux transfer events, which are signatures of pulsed magnetopause reconnection (Russell and Elphic, 1978).

We notice that this auroral configuration consisting of PMAFs/prenoon and PMAFs/postnoon separated by a “midday gap aurora” is consistent with a solar wind-magnetopause-ionosphere coupling which is discontinuous at magnetic noon (see Sandholt and Farrugia, 2003). This is a characteristic feature of the combined antiparallel-component merging configuration described by Fuselier et al. (2011).

A most direct association with magnetopause reconnection in our auroral data (Fig. 5) is the magnetospheric erosion signature seen at 07:40 UT, i.e., the equatorward migration of the green line aurora near the southern horizon. This is due to the disappearance of CPS electrons on newly open field lines, as predicted in the theoretical work of Lockwood (1997). This erosion event is a result of the southward turning of the IMF. This type of auroral erosion effect has also been documented in other cases (see Sandholt and Farrugia, 2002).

4.1.2 Case 3 (ICME): 10 January 2004 ($B_y < 0$; post-noon); convection and S-M effect in response to ICME magnetic field southward turning

On this day, an interplanetary CME was moving over Earth during its radial expansion. An abrupt southward turning of the ICME magnetic field was detected by spacecraft ACE at 13:05 UT when the B_y was negative (-10 nT). This southward turning is marked by the first vertical (dashed) guideline in Fig. 6. A horizontal red line gives the average value of $E_{KL} = (4.0 \pm 0.6)$ mV m⁻¹ in the interval 14:00–18:00 UT. The horizontal red line in the bottom panel gives the average value of Boyle potential = (112.8 ± 3.7) kV.

This gave us a unique chance to study the response in plasma convection in general and the excitation of FC 1-FC 2 flows in the postnoon sector above Svalbard. We shall concentrate on the ground responses in plasma flows and mag-

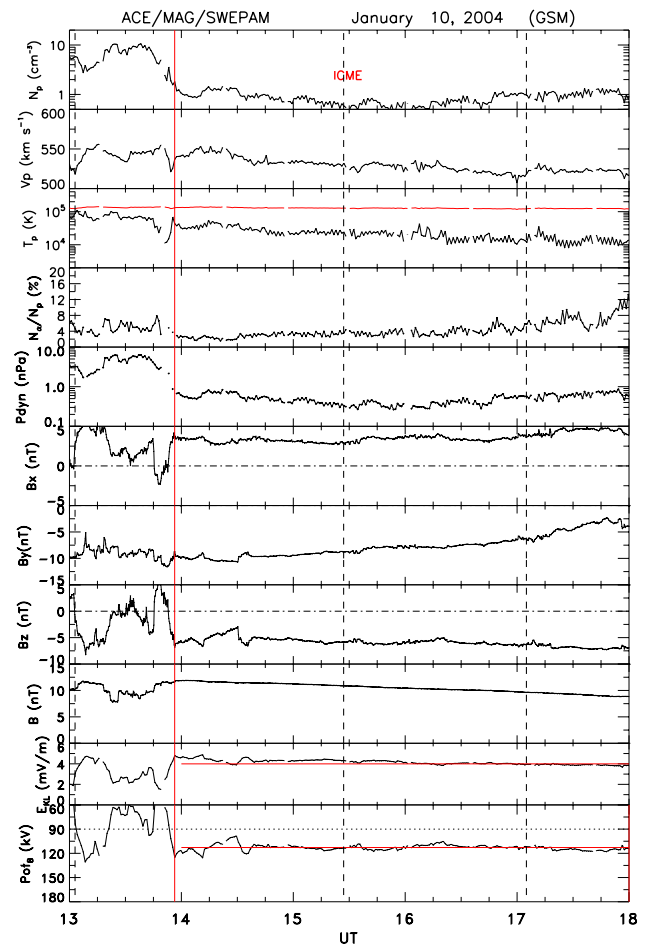


Fig. 6. Interplanetary plasma and magnetic field data obtained from spacecraft ACE during the interval 13:00–18:00 UT on 10 January 2004: proton density, bulk speed and temperature, the alpha-particle-to-proton number density ratios, the dynamic pressure, the components of the magnetic field in GSM coordinates (B_x , B_y , B_z) and the total field strength, the geoeffective interplanetary electric field (E_{KL}) and the Boyle potential (Boyle et al., 1997). Southward turning of the magnetic field at 13:05 UT is marked by the first vertical (dashed) guideline. The vertical dashed lines at 15:27 and 17:05 UT mark the times of F15 passes across flow channel FC 1 in the prenoon sector (approx. 09:00 MLT/70° MLAT), when the ACE to Earth propagation delay is taken into account. The first (vertical) red guideline marks the front boundary of the ICME. The second (horizontal) red line gives the average value of $E_{KL} = (4.0 \pm 0.6)$ mV m⁻¹. The horizontal red line in the bottom panel gives the average value of Boyle potential = (112.8 ± 3.7) kV.

netic deflections to the rapid southward turning of the ICME magnetic field at 13:05 UT.

The second aspect is the study of Birkeland current and ion drift latitude profiles associated with flow channels in prenoon sector (approx. 09:00 MLT/70° MLAT) obtained by satellite F15 during the intervals 16:15–16:17 and 17:58–17:59 UT (see track marked in Fig. 3) which occurred under extremely steady south-west ($B_z < 0$; $B_y < 0$) directed

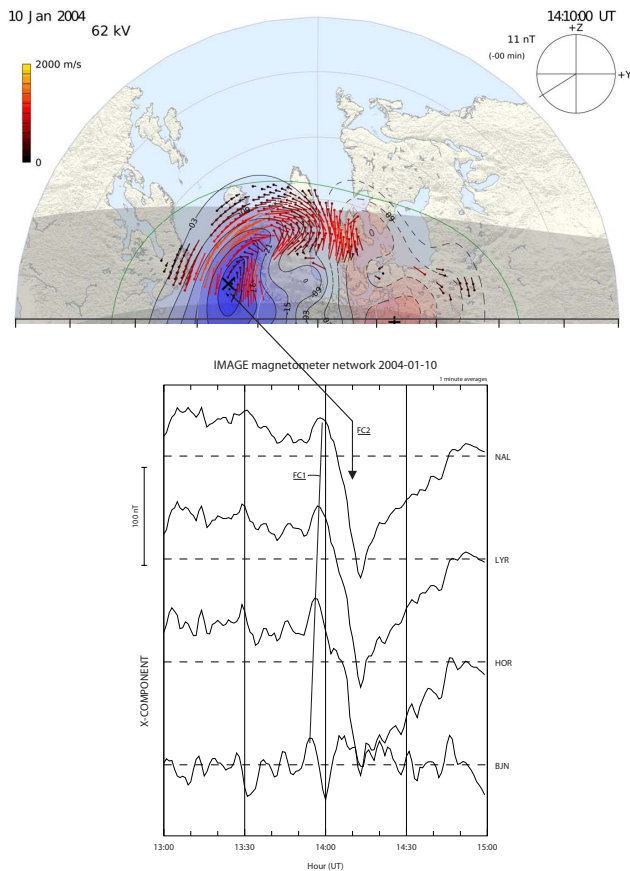


Fig. 7. SuperDARN convection plot for 14:10 UT (top) and ground magnetic deflections from Svalbard IMAGE stations NAL (75° MLAT), LYR (74° MLAT), HOR (73° MLAT) and BJJ (71° MLAT) during the interval 13:00–15:00 UT. Magnetic signatures of enhanced flows in flow channels FC 1 and FC 2 are marked. The coordinate system in the upper panel is MLAT/MLT. The sun is at the top and dusk is to the left. MLAT range from 40° – 90° is shown.

magnetic field conditions. The times of these F15 observations of FC 1/prenoon/ $B_y < 0$ are marked by the last two vertical guidelines in Fig. 6. Here, we assume a propagation delay from ACE to Earth of 50–55 min (see below).

Figure 7 shows the spatial convection plot for 14:10 UT as derived from SuperDARN radars in the upper panel. Flow vectors and convection streamlines are shown (Greenwald et al., 1995; Ruohoniemi and Greenwald, 2005). The coordinate system is MLAT/MLT. MLAT range from 40° – 90° is shown. Flow channels FC 1 and FC 2 are easily identified. Clear FC 2 flows in the form of anti-sunward convection centred at 17:00 MLT/ 75° MLAT are seen above Svalbard. The bottom panel shows four X-component magnetograms from Svalbard stations NAL (75° MLAT), LYR (74° MLAT), HOR (73° MLAT) and BJJ (71° MLAT) during the interval 13:00–15:00 UT. The FC 1 response is seen as a poleward propagating positive X-deflection in the interval 13:50–

14:00 UT. This is followed by an increasing negative deflection in the interval 14:00–14:10 UT. The latter response is the magnetic signature of flow channel FC 2 detected overhead Svalbard by SuperDARN radars. Eastward flow and associated westward Hall current give rise to the negative X-component magnetic deflection. The transition from FC 1 to FC 2 responses at 14:00 UT in the Svalbard stations records is consistent with the polar cap expansion associated with the magnetospheric erosion event initiated by the southward turning of the ICME magnetic field.

The propagation delay between the southward turning recorded by ACE at 13:05 UT and the magnetic signature of the FC 1 flow enhancement at BJJ (13:55 UT) is 50 min.

According to Zhang et al. (2011) the evolution time of FTEs is about 18–22 min from their origin on the magnetopause (at the reconnection site) to the magnetotail lobe. This estimate is consistent with our present observations of the successive FC 1 and FC 2 flow excitations observed during the 20 min long interval from 13:55–14:15 UT in our 10 January 2004 case.

Thus, in this case we identified the B_y -related ground magnetic deflection (Svalgaard-Mansurov effect) associated with enhanced anti-sunward convection in flow channel FC 2 in the postnoon sector under $B_y < 0$ conditions which was initiated by a southward turning of the ICME magnetic field.

4.1.3 Case 4 (ICME): 10 January 2004 ($B_y < 0$; prenoon); convection-precipitation-FAC (Pedersen current closure)

Figure 8 shows data obtained during a pass from pre-midnight (20:00 MLT/ 70° MLAT) to pre-noon (09:00 MLT/ 70° MLAT) indicated in Fig. 3 ($B_y < 0$ /prenoon case). End of the interval of substorm electrojet activity is marked by an arrow in the convection panel. We shall concentrate on the precipitation and FAC structures observed during the traversal of the polar cap boundary in the prenoon sector (09:00 MLT/ 73° – 71°) at 17:58–17:59 UT. FAC polarities are derived from gradients in the B_z -trace. As mentioned above, this pass occurred during a 4-h long interval of very stable, south-west directed ICME magnetic field (Fig. 6). The B_z and B_y components at the time of this pass are very similar (-6 to -7 nT; Fig. 6). We notice the following features:

1. Channel of enhanced anti-sunward flow at polar cap entry at 20 MLT/ 66° MLAT). This occurred at the time of substorm electrojet activity (see Andalsvik et al., 2012, their Fig. 10). It is interpreted as flow channel FC 3 (see Fig. 3), i.e., that flow category which is driven by magnetotail reconnection.
2. Increasing anti-sunward cross-track flow component as the satellite traverses the centre of the polar cap and into the prenoon sector (until approx. 17:55 UT). The reduced polar cap flow speed at 17:55 UT marks the

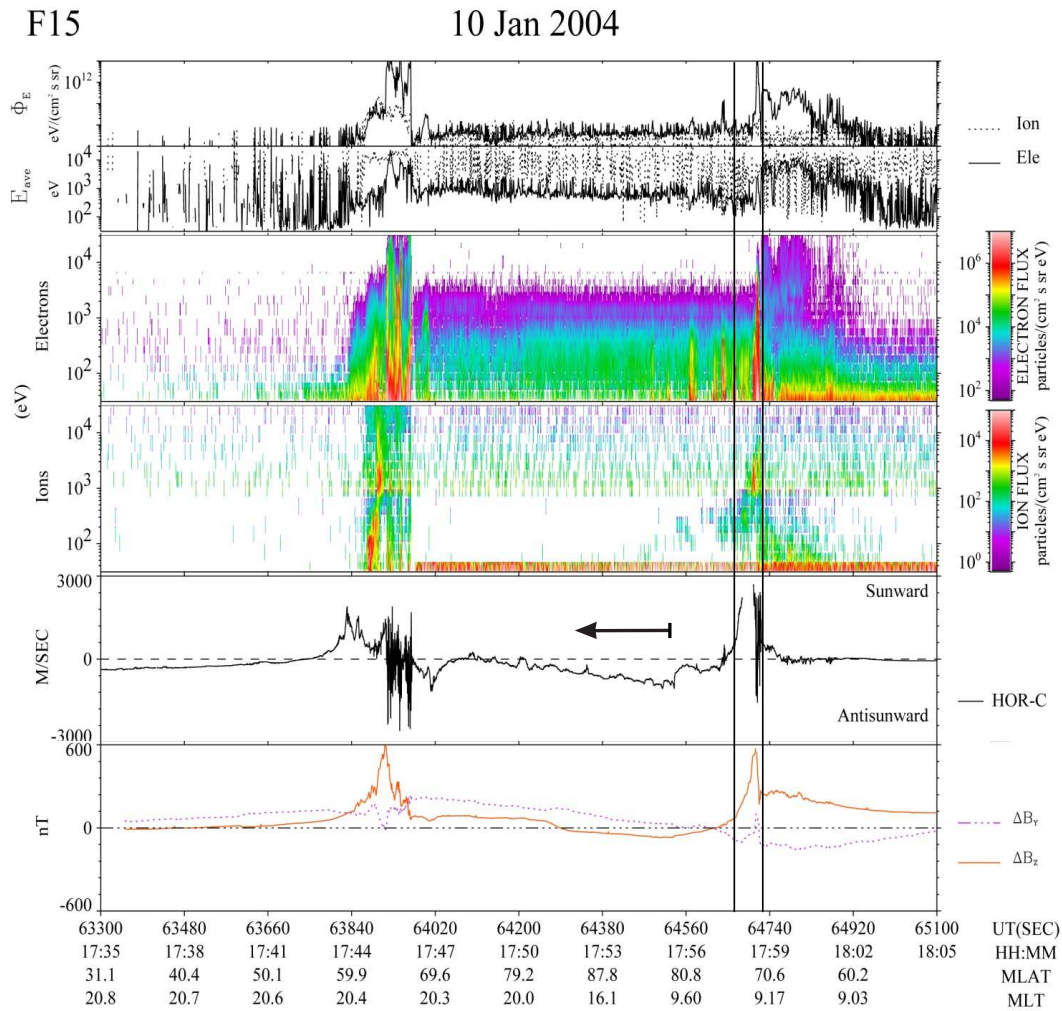


Fig. 8. DMSP F15 data obtained during the pass from pre-midnight to pre-noon MLTs in the interval 17:35–18:05 UT, as indicated in Fig. 3. Panels from top to bottom shows precipitation energy fluxes (ions/electrons), average energies, electron and ion spectrograms, cross-track ion drift, and magnetic deflection components across (B_z ; east-west) and along (B_y) the track. Entry into and subsequent exit of the polar cap occurred at 20:00 MLT/66° MLAT and 09:00 MLT/71° MLAT, respectively. Channel of enhanced sunward convection at 09MLT/71° MLAT is marked by vertical guidelines. End of the interval of substorm electrojet activity is marked by an arrow in the convection panel.

abrupt decay of westward electrojet activity during a substorm (Andalvik et al., 2012).

- Channel of enhanced sunward cross-track flow component at the polar cap boundary is traversed at 17:58 UT (09:00 MLT/71–73° MLAT). This flow channel is bordered on its poleward and equatorward boundaries by inward- and outward-directed FACs, as inferred from positive and negative gradients, respectively, in the B_z -trace in the bottom panel. This is a flow-FAC configuration as marked schematically in the left panel of Fig. 3.
- The equatorward boundary of this flow channel, where the FAC is directed outward, is characterised by enhanced electron precipitation flux (broad energy spectrum) and ion fluxes at 1–3 keV.

- The above mentioned narrow boundary layer flux is located immediately poleward of a latitudinally wide band of CPS electrons.

From these data we conclude that the boundary between the narrow layer of enhanced boundary layer electron energy flux (see spike in the top panel of Fig. 8) and the CPS regime traversed at approx. 17:58:30 UT marks the transition from open to closed field lines. The observed wide-band electron acceleration structure is similar to that documented by Newell et al. (2010). This type of precipitation is referred to by Lockwood (1997) as dayside BPS (newly open field lines) and corresponds to the auroral phenomenon we call PMAFs/prenoon/ $B_y < 0$ (see Sandholt and Farrugia (2007a); their Figs. 7 and 8).

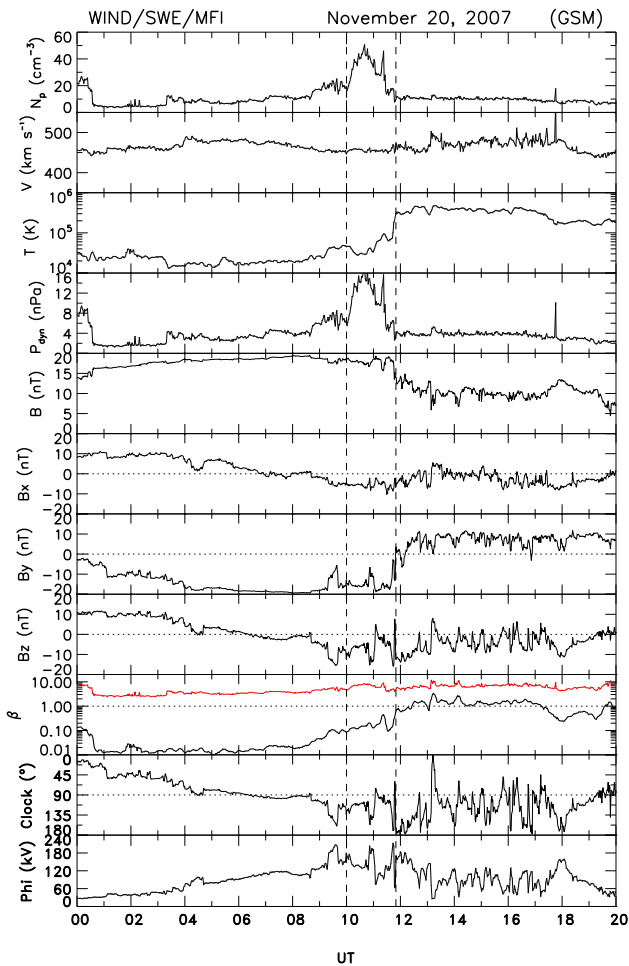


Fig. 9. Wind data for ICME passage at Earth on 20 November 2007. Panels from top to bottom shows: proton density, bulk speed, proton temperature, dynamic pressure, magnetic field components B_x , B_y , B_z , the total field, plasma beta, the clock angle in the GSM Y-Z plane and the Boyle potential. The two vertical guidelines at 10:00 and 11:50 UT mark the interval of polar cap ground magnetic deflections we focus on.

The observation of a relatively good correlation between variations in the cross-track ion drift and the B_z perturbation across the flow channel (see panels five and six in Fig. 8) is as expected for a model describing ionospheric closure of the two FAC sheets by a Pedersen current (Smiddy et al., 1980; Sandholt et al., 1989). Deviations from such a correlation are usually attributed to the presence of conductivity gradients and associated polarization electric fields.

4.1.4 Case 5 (ICME): 20 November 2007 ($B_y < 0$; post-noon); pulsed flows and S-M effect

Figure 9 shows interplanetary plasma and magnetic field data for the ICME passage at Earth on 20 November 2007. Wind was situated at $(236, 86, 16) R_E$ at 04:00 UT, 20 November and the Wind-Earth propagation delay is ~ 1 h. We shall con-

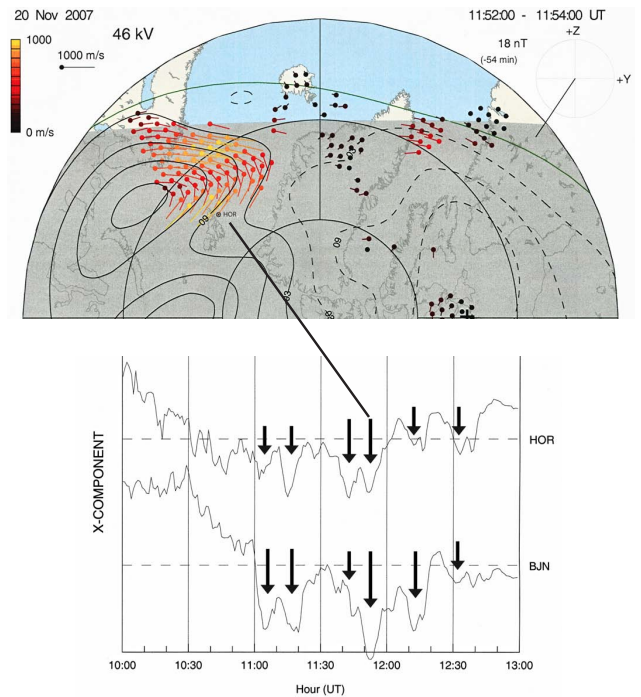


Fig. 10. SuperDARN convection plot for 11:52–11:54 UT (top) and ground magnetic perturbations (marked by arrows) in two Svalbard stations (HOR and BJN) during the interval 10:00–13:00 UT.

centrate on the south-west directed ($B_z < 0$; $B_y < 0$) field near the trailing edge of the ICME detected by Wind during the interval 10:00–11:50 UT. This interval is characterised by an initial rise and a subsequent fall of the dynamic pressure from 6–16–4 nPa. The dynamic pressure variation and the variable magnetopause reconnection rate contributed to expansions/contractions of the polar cap during the interval 10:30–12:40 UT. As a result of this reconnection rate variability (see e.g., southward turning of the ICME magnetic field at $\sim 09:30$ UT; Wind time) and dynamic pressure variations (e.g., enhancement at 10:00 UT; Wind time), with associated polar cap boundary motions, Svalbard magnetometer stations were in the right position (70 – 75° MLAT) to detect the magnetic signatures of episodic enhancements of anti-sunward polar cap convection (flow channel FC 2) during the interval 11:00–12:40 UT.

The interval is characterised by a high level of polar cap convection (polar cap potential drop) and its variability, driven by dayside reconnection, as estimated from the Boyle potential (Boyle et al., 1997), which is fluctuating between 100–180 kV.

Figure 10 shows SuperDARN convection plot for 11:52–11:54 UT (top) and ground magnetic perturbations in Svalbard during the interval 10:00–13:00 UT. The ground stations are HOR (74° MLAT) and BJN (71° MLAT). In the SuperDARN plot we distinguish between two flow stages, i.e., northwestward flows (our FC 1) centred at approx.

70° MLAT, and anti-sunward flows (our FC 2) at higher latitudes (71–75° MLAT; approx. 15:00 MLT), where the Svalbard stations (e.g., HOR at 74° MLAT) are located. The tilted line connecting the two panels of the figure marks the association between anti-sunward flow in FC 2 and the magnetic deflection at station HOR at 11:52 UT.

In Fig. 10 we, therefore, illustrate the ground magnetic deflections in the regime of flow channel FC 2. This appears as a series of negative X-deflections in the HOR (74° MLAT) and BJN (71° MLAT) magnetograms in the regime of enhanced anti-sunward convection, as detected by SuperDARN radars. The most clear magnetic events are observed during the interval 11:00–12:40 UT. The end of the events series at 12:40 UT corresponds to the ICME B_y field polarity transition from negative to positive recorded by Wind approx. 50 min earlier (at 11:50 UT).

In our view this series of negative X-component deflections is a Svalgaard-Mansurov effect corresponding to the tailward evolution of open flux tubes along the duskside periphery of the polar cap, associated with flux transfer events, as predicted by Southwood (1987) for the prevailing $B_y < 0$ conditions of the actual ICME field (Sandholt et al., 2010b). After 12:40 UT, when B_y is positive, the Svalgaard-Mansurov effect is presumably shifted to the prenoon sector of the polar cap.

By this case, we demonstrate a temporal structure of the Svalgaard-Mansurov effect associated with pulsed anti-sunward convection in the regime of flow channel FC 2.

5 Flow channel FC 2 and IMF-magnetosphere interconnection topology

Figure 11 shows a schematic illustration of IMF-magnetosphere interconnection topology for a southwest-directed ($B_z < 0$; $B_y < 0$) IMF. The figure shows the GSM Y-Z plane along the dawn-dusk meridian ($X = 0$). The emphasis is on 4-component sheets of field-aligned electric currents (C1-C2-R1-R2) and flow channel FC 2 located on old open field lines (downstreamside of the cusp). The current circuit involving Birkeland currents C1-C2 (marked blue) consists of C1-C2 with ionospheric Pedersen current closure (not shown) and the tail magnetopause current. The C2 current represents the outer layer (poleward part) of the R1 current which is connected to the outer part of the LLBL (open field lines). This is the “extra downstreamside cleft-associated R1 current” of Watanabe et al. (1996). Our C1 current is the “extra R0 current” of Watanabe et al. (1996).

Flow channel FC 1 (not shown in this figure) is the result of ionospheric Pedersen current closure of the dayside R1 FAC residing on newly open field lines, as illustrated by Figs. 4 and 8.

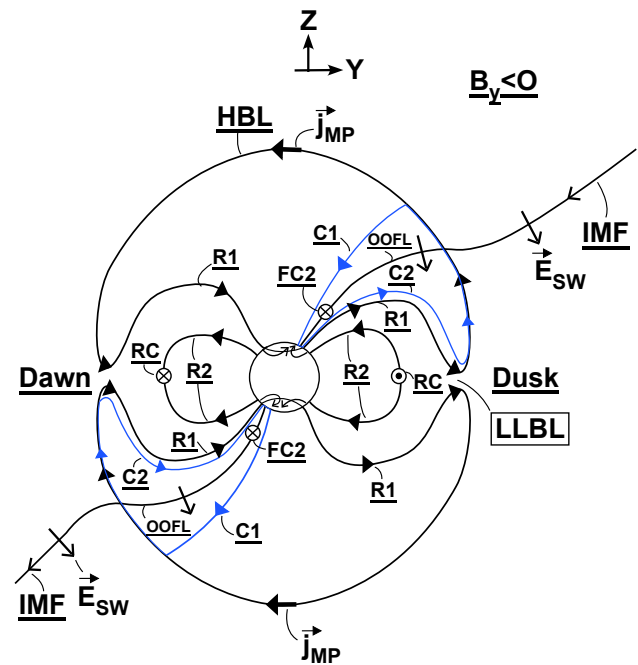


Fig. 11. Schematic IMF-magnetosphere-ionosphere interconnection topology in stage two of the open field line evolution for southwest-directed IMF ($B_z < 0$; $B_y < 0$) conditions. The emphasis here is on old open field lines (OOFLs), sheets of field-aligned electric currents (C1-C2-R1-R2) and flow channel FC 2. Current circuit involving Birkeland currents C1-C2 are marked in blue. The figure shows the GSM Y-Z plane along the dawn-dusk meridian ($X = 0$). Dusk is to the right. North is up.

6 Summary and conclusions

In our review of recent statistical and event studies we aim at shedding light on the spatial-temporal structure of plasma convection, FACs, precipitation/aurora and associated ground magnetic deflections in the polar cap. The emphasis is on spatial-temporal structure of FACs and convection as origin of the S-M effect in ground magnetic deflections, i.e., the increased (decreased) H-component appearing in away (toward) sectors of the IMF, as illustrated in our case example shown in Fig. 2. To this end, we distinguish between S-M effects in two stages of evolution of open field lines in the Dungey model of plasma convection in the reconnecting magnetosphere.

The basis for this inference is our documentation that both flow channels FC 1 and FC 2 are essential elements in the temporal-spatial structure of Dungey convection cells. First of all, we argue that it is most appropriate to distinguish between these two convection stages. This is demonstrated, for example, by the sequential activations of these flows during the first approx. 20 min after southward turnings of the IMF, as illustrated in Fig. 7. Furthermore, we find that the two flow features correspond to ionospheric Pedersen current closures of two specific FAC pairs related to different spatial-temporal

domains of the solar wind-magnetosphere-ionosphere interconnection topology, as shown in Fig. 4.

FC 1 is a flow channel located on newly open field lines appearing on either side of noon for a given IMF B_y polarity. Both the prenoon and postnoon channels are closely connected with specific auroral phenomena, namely, poleward-moving auroral forms (PMAFs/prenoon and PMAFs/postnoon) (Sandholt and Farrugia, 2007a). The regime of the outward-directed FAC component at the equatorward (poleward) border of FC 1/prenoon (postnoon) is characterised by accelerated electrons and associated intense auroral emissions at 557.7 and 630.0 nm. This precipitation regime is the dayside BPS precipitation on newly open field lines, as described by Lockwood (1997). A good example of the FC 1/ $B_y < 0$ /prenoon variant, observed during extremely steady interplanetary CME conditions, is given in Fig. 8.

For a given B_y polarity FC 1-PMAFs/prenoon and FC 1-PMAFs/postnoon are separated by a diminution of auroral activity around noon, the “midday gap aurora” (see Fig. 5). This auroral configuration is consistent with solar wind-magnetopause-ionosphere coupling processes which are discontinuous at noon, as is also argued by e.g., Sandholt and Farrugia (2003) and Fuselier et al. (2011).

Our inferences on these aurora-convection-FAC configurations in the vicinity of the open/closed field line boundary are largely based on previous documentation of the correspondence between auroral forms and particle precipitation regimes (Newell and Meng, 1994; Lockwood, 1997): CPS-void-dayside BPS/LLBL (see, e.g., Sandholt and Newell, 1992; Sandholt and Farrugia, 2002; Sandholt et al., 2004). Additional relevant information is obtained from auroral signatures of magnetopause reconnection events excited by rapid southward turnings of the IMF, which are characterised by (i) disappearance (equatorward shift) of a diffuse green line aurora excited by magnetospheric (CPS) electrons, and (ii) appearance of dayside BPS aurora (PMAFs) associated with the presence of accelerated magnetosheath electrons (Sandholt and Farrugia, 2002), as predicted by Lockwood (1997).

In contrast to FC 1, FC 2 is a flow channel located on old open field lines on the downstream side of the cusp (Farrugia et al., 2004). The FC 2 flow channel shows a characteristic prenoon-postnoon asymmetry (Fig. 3). It is mainly located on the postnoon/dusk (prenoon/dawn) side of the polar cap for IMF $B_y < 0$ (> 0) conditions. We identified this flow channel (FC 2) in the equivalent convection derived from Weimer patterns of ground magnetic deflections (Weimer et al., 2010). This inference is based on the well-known association between ionospheric Hall currents and ground magnetic deflections (Fukushima, 1969). Thus, the IMF B_y -related FC 2 flows are accompanied by ionospheric Hall currents which give rise to a Svalgaard-Mansurov effect since the current is eastward-directed for $B_y > 0$ and westward-directed for $B_y < 0$. This S-M effect is connected to the ionospheric Pedersen current closure of the C1-C2 cur-

rents depicted in Fig. 11 and described by Watanabe as “extra downstreamside cleft-associated region 1” (C2) and “extra region 0” (C1) currents. Our FC 2 flow channel is included in the regime of the polar electrojet (PE), applying the terminology of Feldstein et al. (2006) (see their Fig. 15d, e).

The central point in our reasoning, as illustrated in our Figs. 4 ($B_y > 0$ case) and 8 ($B_y < 0$ case), is that the dayside R1 current is split into two components (current sheets). The northernmost FAC sheet (our C2 current) is connected to the high-altitude solar wind-magnetosphere dynamo current on the downstreamside of the cusp. The other circuit elements are the ionospheric Pedersen current closure and the high-latitude FAC we call C1. This current circuit is responsible for momentum transfer to the ionosphere in the second stage of evolution of open field lines in the Dungey cycle, i.e., during the interval when time elapsed since magnetopause reconnection is approx. 10–20 min. This is in contrast to the dayside R1 current which belongs to the regime of newly open field lines. Thus, the boundary between the R1 and C2 current regimes is characterised by a jump in the low-energy ion cutoff (time elapsed since reconnection), as demonstrated in our Fig. 4. We note that the distinction between the R1 and C2 currents appears in case studies (Sandholt and Newell, 1992; Farrugia et al., 2003, 2004), but not in large statistical studies of FACs, due to smoothing effects (see e.g., Anderson et al., 2008).

The outward-directed FAC (C2) at the equatorward boundary of the dusk-side ($B_y < 0$) FC 2 is accompanied by electron precipitation structures with energy extending to approx. 1 keV (flank LLBL source), giving rise to discrete auroral forms in the close vicinity of the polar cap boundary (Sandholt and Farrugia, 2007a).

In combined observations of convection and ground magnetic deflections obtained by SuperDARN and the IMAGE Svalbard chain of magnetometer data, we document in Fig. 10 a sequence of 5–10 min long ground magnetic deflections at polar cap latitudes, within the FC 2 regime. In our view, this is a temporal structure of the S-M effect related to pulsed anti-sunward convection. This type of pulsed flows along the periphery of the polar cap was predicted by Southwood (1987) as an ionospheric signature of flux transfer events, which result from pulsed magnetopause reconnection. Thus, we document in Fig. 10 the presence of a clear manifestation of flux transfer events (modulations of the magnetopause reconnection rate) in the S-M effect for the case of $B_y < 0$ conditions.

In summary, to fully appreciate the sources of the S-M magnetic fluctuations, one needs to consider the FACs related to both newly open and old open field lines and the strong Hall currents flowing in the respective flow channels formed by their ionospheric Pedersen current closures.

Acknowledgements. Access to the DMSP data base (<https://swx.plh.af.mil>) was kindly provided by Air Force Geophysics Research

Laboratory, Hanscom, Mass through Gordon Wilson. Ground magnetograms from the Svalbard IMAGE chain of ground stations were obtained from <http://www.geo.fmi.fi/image>. We thank Ari Viljanen and Truls Lynne Hansen for IMAGE chain magnetograms and W. Denig for providing high-quality DMSP F15 data used in Fig. 8. We thank M. Ruohoniemi and the SuperDARN team for the convection plots. Work at University of Oslo is supported by the Norwegian Research Council (NFR). Work at UNH is supported by NASA grant NNX10AQ29G.

Topical Editor I. A. Daglis thanks two anonymous referees for their help in evaluating this paper.

References

- Andalsvik, Y., Sandholt, P. E., and Farrugia, C. J.: Substorms and polar cap convection: the 10 January 2004 interplanetary CME case, *Ann. Geophys.*, 30, 67–80, doi:10.5194/angeo-30-67-2012, 2012.
- Anderson, B. J., Korth, H., Waters, C. L., Green, D. L., and Stauning, P.: Statistical Birkeland current distributions from magnetic field observations by the Iridium constellation, *Ann. Geophys.*, 26, 671–687, doi:10.5194/angeo-26-671-2008, 2008.
- Boyle, C. B., Reiff, P. H., and Hairston, M. R.: Empirical polar cap potentials, *J. Geophys. Res.*, 102, 111–125, 1997.
- Burlaga, L. F., Sittler, E., Mariani, F., and Schwenn, R.: Magnetic loop behind an interplanetary shock: Voyager, Helios, and IMP-8 observations, *J. Geophys. Res.*, 86, 6673–6684, 1981.
- Denig, W. F., Burke, W. J., Maynard, N. C., Rich, F. J., Jacobsen, B., Sandholt, P. E., Egeland, A., Leontjev, S., and Vorobjev, V. G.: Ionospheric signatures of dayside magnetopause transients: A case study using satellite and ground measurements, *J. Geophys. Res.*, 98, 5969–5980, 1993.
- Escoubet, C. P., Smith, M. F., Fung, S. F., Anderson, P. C., Hoffman, R. A., Basinska, E. M., and Bosqued, J. M.: Staircase ion signature in the polar cusp: A case study, *Geophys. Res. Lett.*, 19, 1735–1738, 1992.
- Farrugia, C. J., Sandholt, P. E., Maynard, N. C., Torbert, R. B., and Ober, D. M.: Temporal variations in a four-sheet field-aligned current system and associated aurorae as observed during a Polar-ground magnetic conjunction in the midmorning sector, *J. Geophys. Res.*, 108, 1230, doi:10.1029/2002JA009619, 2003.
- Farrugia, C. J., Lund, E. J., Sandholt, P. E., Wild, J. A., Cowley, S. W. H., Balogh, A., Mouikis, C., Möbius, E., Dunlop, M. W., Bosqued, J.-M., Carlson, C. W., Parks, G. K., Cerisier, J.-C., Kelly, J. D., Sauvaud, J.-A., and Rème, H.: Pulsed flows at the high-altitude cusp poleward boundary, and associated ionospheric convection and particle signatures, during a Cluster – FAST – SuperDARN – Søndrestrøm conjunction under a southwest IMF, *Ann. Geophys.*, 22, 2891–2905, doi:10.5194/angeo-22-2891-2004, 2004.
- Farrugia, C. J., Matsui, H., Kucharek, H., Torbert, R. B., Smith, C. W., Jordanova, V. K., Ogilvie, K. W., Lepping, R. P., Berdichevsky, D. B., Terasawa, T., Kasper, J., Mukai, T., Saito, Y., and Skoug, R.: Interplanetary coronal mass ejection and ambient interplanetary magnetic field correlations during the Sun–Earth connection events of October–November 2003, *J. Geophys. Res.*, 110, A09S13, doi:10.1029/2004JA010968, 2005.
- Feldstein, Y. I., Popov, V. A., Cumnock, J. A., Prigancova, A., Blomberg, L. G., Kozyra, J. U., Tsurutani, B. T., Gromova, L. I., and Levitin, A. E.: Auroral electrojets and boundaries of plasma domains in the magnetosphere during magnetically disturbed intervals, *Ann. Geophys.*, 24, 2243–2276, doi:10.5194/angeo-24-2243-2006, 2006.
- Friis-Christensen, E., Lassen, K., Wiljelm, J., Wilcox, J. M., Gonzales, W., and Colburn, D. S.: Critical component of the interplanetary magnetic field responsible for the large geomagnetic effects in the polar cap, *J. Geophys. Res.*, 77, 3371–3376, 1972.
- Fukushima, N.: Equivalence in ground geomagnetic effect of Chapman-Vestine and Birkeland-Alfvén electric current systems for polar magnetic storms, *Rep. Ionos. Space Res. Jap.*, 23, 219–227, 1969.
- Fuselier, S. A., Trattner, K. J., and Petrinec, S. M.: Antiparallel and component reconnection at the dayside magnetopause, *J. Geophys. Res.*, 116, A10227, doi:10.1029/2011JA016888, 2011.
- Greenwald, R. A., Baker, K., Dudeney, J. R., Pinnock, M., Thomas, E. C., Villain, J. P., Cerisier, J.-C., Senior, C., Hanuise, C., Hunsucker, R. D., Sofko, G. J., Koehler, J., Nielsen, E., Pellinen, R., Walker, A. D. M., Sato, N., and Yamagishi, H.: DARN/SUPERDARN: A Global View of the Dynamics of High-Latitude Convection, *Space Sci. Rev.*, 71, 761–796, 1995.
- Howard, R. A., Michels, D. J., Sheeley Jr., N. R., and Koomen, M. J.: The observation of a coronal transient directed at Earth, *Astrophys. J.*, 263, L101–L104, 1982.
- Janzhura, A. S. and Troshichev, O. A.: Identification of the IMF sector structure in near-real time by ground magnetic data, *Ann. Geophys.*, 29, 1491–1500, doi:10.5194/angeo-29-1491-2011, 2011.
- Jørgensen, T. S., Friis-Christensen, E., and Wilhelm, J.: Interplanetary magnetic field direction and high-latitude ionospheric currents, *J. Geophys. Res.*, 77, 1976–1977, 1972.
- Lepping, R. P., Berdichevsky, D. B., and Wu, C.-C.: Sun–Earth electrodynamics: The solar wind connection, *Recent Res. Devel. Astrophys.*, 1, 139–171, 2003.
- Lockwood, M.: Relationship of dayside auroral precipitations to the open-closed separatrix and the pattern of convective flow, *J. Geophys. Res.*, 102, 17475–17487, 1997.
- Lockwood, M., Denig, W. F., Farmer, A. D., Davda, V. N., Cowley, S. W. H., and Luhr, H.: Ionospheric signatures of pulsed reconnection at the Earth’s magnetopause, *Nature*, 361, 424–428, 1993.
- Mansurov, S. M.: New evidence of the relationship between magnetic field in space and on the earth, *Geomagn. Aeron. (Engl. translation)*, 9, 768–773, 1969.
- Newell, P. T. and Meng, C.-I.: Ionospheric projection of magnetospheric regions under low and high solar wind pressure conditions, *J. Geophys. Res.*, 99, 273–286, 1994.
- Newell, P., Lee, A. R., Liou, K., Wing, S., Ohtani, S., Wing, S., and Hairston, M.: Multisatellite low-altitude observations of a magnetopause merging burst, *J. Geophys. Res.*, 115, A11204, doi:10.1029/2010JA015438, 2010.
- Potemra, T. A.: Sources of large-scale Birkeland currents, in: *Physical Signatures of Magnetospheric Boundary Layer Processes*, NATO ASI Series C, vol. 425, pp. 3–27, Kluwer Academic Publishers, Dordrecht, Holland, 1994.
- Ruohoniemi, J. M., and Greenwald, R. A.: Dependencies of high-latitude plasma convection: Consideration of interplanetary magnetic field, season, and universal time factors in statistical patterns, *J. Geophys. Res.*, 110, A09204,

- doi:10.1029/2004JA010815, 2005.
- Russell, C. T. and Elphic, R. C.: Initial ISEE magnetometer results: Magnetopause observations, *Space Sci. Rev.*, 22, 681–715, 1978.
- Sandholt, P. E. and Farrugia, C. J.: Monitoring magnetosheath-magnetosphere interconnection topology from the aurora, *Ann. Geophys.*, 20, 629–637, doi:10.5194/angeo-20-629-2002, 2002.
- Sandholt, P. E. and Farrugia, C. J.: Does the aurora provide evidence for the occurrence of antiparallel magnetopause reconnection?, *J. Geophys. Res.*, 108, 1466, doi:10.1029/2003JA010066, 2003.
- Sandholt, P. E. and Farrugia, C. J.: Poleward moving auroral forms (PMAFs) revisited: responses of aurorae, plasma convection and Birkeland currents in the pre- and postnoon sectors under positive and negative IMF B_y conditions, *Ann. Geophys.*, 25, 1629–1652, doi:10.5194/angeo-25-1629-2007, 2007a.
- Sandholt, P. E. and Farrugia, C. J.: The role of poleward moving auroral forms in the dawn-dusk precipitation asymmetries induced by IMF B_y , *J. Geophys. Res.*, 112, A04203, doi:10.1029/2006JA011952, 2007b.
- Sandholt, P. E. and Farrugia, C. J.: Plasma flow channels at the dawn/dusk polar cap boundaries: momentum transfer on old open field lines and the roles of IMF B_y and conductivity gradients, *Ann. Geophys.*, 27, 1527–1554, doi:10.5194/angeo-27-1527-2009, 2009.
- Sandholt, P. E. and Newell, P. T.: Ground and satellite observations of an auroral event at the cusp/cleft equatorward boundary, *J. Geophys. Res.*, 97, 8685–8691, 1992.
- Sandholt, P. E., Egeland, A., Holtet, J. A., Lybakk, B., Svenes, K., Åsheim, S., and Deehr, C. S.: Large- and small-scale dynamics of the polar cusp, *J. Geophys. Res.*, 90, 4407–4414, 1985.
- Sandholt, P. E., Jacobsen, B., Lybakk, B., Egeland, A., Bythrow, P. F., and Hardy, D. A.: Electrodynamics of the polar cusp ionosphere: A case study, *J. Geophys. Res.*, 94, 6713–6722, 1989.
- Sandholt, P. E., Moen, J., and Opsvik, D.: Periodic auroral events at the midday polar cap boundary: implications for solar wind-magnetosphere coupling, *Geophys. Res. Lett.*, 19, 1223–1226, 1992.
- Sandholt, P. E., Denig, W. F., Farrugia, C. J., Lybakk, B., and Trondsen, E.: Auroral structure at the cusp equatorward boundary: Relationship with the electron edge of low-latitude boundary layer precipitation, *J. Geophys. Res.*, 107, 1235, doi:10.1029/2001JA005081, 2002.
- Sandholt, P. E., Farrugia, C. J., and Denig, W. F.: Dayside aurora and the role of IMF $|B_y|/|B_z|$: detailed morphology and response to magnetopause reconnection, *Ann. Geophys.*, 22, 613–628, doi:10.5194/angeo-22-613-2004, 2004.
- Sandholt, P. E., Andalsvik, Y., and Farrugia, C. J.: Polar cap flow channel events: spontaneous and driven responses, *Ann. Geophys.*, 28, 2015–2025, doi:10.5194/angeo-28-2015-2010, 2010a.
- Sandholt, P. E., Andalsvik, Y., and Farrugia, C. J.: Polar cap convection/precipitation states during Earth passage of two ICMEs at solar minimum, *Ann. Geophys.*, 28, 1023–1042, doi:10.5194/angeo-28-1023-2010, 2010b.
- Smiddy, M., Burke, W. J., Kelley, M. C., Saffekos, N. A., Gussenhoven, M. S., Hardy, D. A., and Rich, F. J.: Effects of high-latitude conductivity on observed convection electric fields and Birkeland currents, *J. Geophys. Res.*, 85, 6811–6818, 1980.
- Sonnerup, B. U. O. and Siebert, K. D.: Theory of the low-latitude boundary layer and its coupling to the ionosphere: A tutorial review, in: *Earth's Low-Latitude Boundary Layer*, Geophysical Monograph, vol. 133, edited by: Newell, P. T. and Onsager, T., pp. 13–32, American Geophysical Union, Washington, D.C., 2003.
- Southwood, D. J.: The ionospheric signature of flux transfer events, *J. Geophys. Res.*, 92, 3207–3213, 1987.
- Svalgaard, L.: Sector structure of the interplanetary magnetic field and daily variation of the geomagnetic field at high latitudes, *Det Danske Meteorologiske institutt, Charlottenlund*, Preprint R-6, 1968.
- Svalgaard, L.: Polar cap magnetic variations and their relationship with the interplanetary magnetic sector structure, *J. Geophys. Res.*, 78, 2064–2078, 1973.
- Taguchi, S., Sugiura, M., Winningham, J. D., and Slavin, J.: Characterization of the IMF B_y -dependent field-aligned currents in the cleft region based on DE 2 observations, *J. Geophys. Res.*, 98, 1393–1407, 1993.
- Troshichev, O. A., Lukianova, R. Y., Papitashvili, V. O., Rich, F. J., and Rasmussen, O.: Polar cap index (PC) as a proxy for ionospheric electric field in the near-pole region, *Geophys. Res. Lett.*, 27, 23, doi:10.1029/2000GL003756, 2000.
- Watanabe, M., Iijima, T., and Rich, F. J.: Synthesis models of dayside field-aligned currents for strong interplanetary magnetic field B_y , *J. Geophys. Res.*, 101, 13303–13319, 1996.
- Weimer, D. R., Clauer, C. R., Engebretson, M. J., Hansen, T. L., Gleisner, H., Mann, I., and Yumoto, K.: Statistical maps of geomagnetic perturbations as a function of the interplanetary magnetic field, *J. Geophys. Res.*, 115, A10320, doi:10.1029/2010JA015540, 2010.
- Wing, S., Ohtani, S.-I., Newell, P. T., Higuchi, T., Ueno, G., and Weygand, J. M.: Dayside field-aligned current source regions, *J. Geophys. Res.*, 115, A12215, doi:10.1029/2010JA015837, 2010.
- Zhang, Q.-H., Dunlop, M. W., Liu, R.-Y., Yang, H.-G., Hu, H.-Q., Zhang, B.-C., Lester, M., Bogdanova, Y. V., McCrea, I. W., Hu, Z.-J., Crothers, S. R., La Hoz, C., and Nielsen, C. P.: Coordinated Cluster/Double Star and ground-based observations of dayside reconnection signatures on 11 February 2004, *Ann. Geophys.*, 29, 1827–1847, doi:10.5194/angeo-29-1827-2011, 2011.